

**Impact of image averaging on wide-field choroidal thickness measurements using enhanced-depth imaging optical coherence tomography**

**Author**

Hoseini-Yazdi, Hosein, Vincent, Stephen J, Collins, Michael J, Read, Scott A, Alonso-Caneiro, David

**Published**

2019

**Journal Title**

Clinical and Experimental Optometry

**Version**

Accepted Manuscript (AM)

**DOI**

[10.1111/cxo.12855](https://doi.org/10.1111/cxo.12855)

**Downloaded from**

<http://hdl.handle.net/10072/383690>

**Griffith Research Online**

<https://research-repository.griffith.edu.au>

## RESEARCH

Impact of image averaging on wide-field choroidal thickness measurements using enhanced-depth imaging optical coherence tomography

Hosein Hoseini-Yazdi\* PhD

Stephen J Vincent\* PhD

Michael J Collins\* PhD

Scott A Read\* PhD

David Alonso-Caneiro\* PhD

\*Contact Lens and Visual Optics Laboratory, School of Optometry and Vision Science, Queensland University of Technology, Brisbane, Australia

Running title: Choroidal thickness variations with B-scan averaging

**Key words:** choroidal thickness, enhanced-depth imaging, B-scan averaging, optical coherence tomography, wide-field imaging

**Background:** To examine the influence of B-scan averaging on choroidal thickness using wide-field enhanced-depth imaging optical coherence tomography.

**Methods:** Six high-resolution trans-foveal horizontal enhanced-depth imaging line scans (spanning a 60° field) were acquired consecutively from the right eye of 10 healthy adults (mean age  $30 \pm 5$  years), with each line scan an average of 10, 20, 30, 40, 50 or 100 B-scans using the automated real time image averaging and follow-up features of the Spectralis device. The impact of B-scan averaging on regional measures of wide-field choroidal thickness (across macular and peripheral regions) and their accuracy was investigated, assuming that averaging 100 B-scans would provide the most accurate estimate of choroidal thickness.

**Results:** Regional estimates of wide-field choroidal thickness did not vary across the different B-scan averaging conditions (all  $p > 0.05$ ). The mean choroidal thickness averaged across the full wide-field area exhibited the closest agreement to measures obtained with 100 averaged B-scans when frame averaging exceeded 30 B-scans (95% limits of agreement +10 to -7, +7 to -7, and +6 to -3  $\mu\text{m}$  for 30, 40, and 50 averaged B-scans respectively), compared to 10 and 20 averaged B-scans (95% limits of agreement +13 to -8, and +13 to -6  $\mu\text{m}$ , respectively;  $p < 0.01$  and  $p < 0.02$  compared to the accuracy of 50 averaged B-scans).

**Conclusion:** Averaging 30 B-scans for an individual enhanced-depth imaging optical coherence tomography line scan provided accurate measures of choroidal thickness across a wide-field (60°) area in young healthy eyes. This information is important for designing the volumetric scan protocols required for detailed examination of the macular and peripheral choroid.

The thickness of the choroid varies regionally across the macular<sup>1</sup> and peripheral regions.<sup>2-4</sup> Further, structural changes in the choroid across a wide-field may contribute to the pathophysiology of a range of ocular conditions including myopia,<sup>4</sup> age-related macular degeneration,<sup>3</sup> central serous chorioretinopathy,<sup>5</sup> and glaucoma.<sup>6</sup> Therefore, the use of wide-field volumetric enhanced-depth imaging optical coherence tomography (EDI-OCT) for imaging of the choroid may be important for improving the diagnosis and monitoring of numerous ocular conditions. Given the typically longer acquisition time for wide-field volumetric OCT scanning protocols, conventional choroidal imaging techniques used for the central macular regions need to be optimised for imaging the central and peripheral choroid. Averaging multiple B-scan images is an important component of OCT imaging of the choroid, since it improves the signal to noise ratio, allowing more reliable visualization of the choriocleral interface.<sup>7</sup> While using the maximum possible number of frames for B-scan averaging (100 B-scans) is desirable to reduce noise and optimise the visibility of the choroid, it also increases the scan duration, and the likelihood of greater subject fatigue and eye movements during image acquisition.

The optimum number of frames for image averaging during OCT imaging of the retina has been investigated based on objective<sup>8-10</sup> and subjective<sup>11</sup> determination of the improvement in a range of image quality parameters including image brightness, layer contrast, and noise variance. Averaging 16 to 20 B-scans significantly improves image quality metrics compared to a single non-averaged image, with further increases in the number of frames for B-scan averaging not significantly enhancing the image quality. However, there is a paucity of knowledge regarding the effect of image averaging on choroidal thickness measurements across the macular and peripheral regions.

This study was designed to examine the number of averaged B-scans required to optimise measures of wide-field choroidal thickness. The impact of image averaging on short-term variations in regional choroidal thickness measurements was examined. Further, the agreement between the average wide-field choroidal thickness measurements using different frame averaging conditions and measurements obtained using 100 averaged B-scans were investigated, assuming that averaging the maximum number of B-scans would provide the most accurate estimate of the choroidal thickness.

## **METHODS**

### **Subjects**

Ten healthy young adults with a mean age of  $30 \pm 5$  years, and a mean refractive error of  $-0.82 \pm 1.76$  D (range  $-4.75$  to  $+0.75$  D, 3 myopes and 7 emmetropes) were recruited from the students and staff of the Queensland University of Technology (QUT), Brisbane, Australia. Written informed consent was obtained from all participants and the study procedures adhered to the tenets of the Declaration of Helsinki and were approved by the QUT human research ethics committee.

The refractive error and ocular health of the participants were assessed using non-cycloplegic subjective refraction and slit lamp examination in order to include subjects with less than  $-6.00$  D of myopia,  $+1.00$  D of hyperopia, and  $1.00$  D of astigmatism without any systemic or ocular pathology. No participants exhibited any history of past ocular surgery and were not using any systemic or topical medications known to affect the choroid. Since choroidal thickness may vary with smoking,<sup>12</sup> consumption of coffee,<sup>13</sup> and alcohol,<sup>14</sup> only non-smokers were included in this experiment and participants refrained from coffee or alcohol intake for at least four hours prior to the study visit. Subjects who were undergoing myopia control treatments such as orthokeratology, multifocal spectacle or contact lens or atropine therapy were excluded due to possible effect of these treatments on choroidal thickness.<sup>15, 16</sup>

Subjects completed a 20-minute “wash-out” period while seated watching a movie at a five metre distance before the acquisition of OCT images in order to minimise the influence of prior near tasks<sup>17</sup> and physical activity<sup>18</sup> on choroidal thickness. Given the potential effects of ambient light intensity on the choroidal thickness,<sup>19</sup> ambient room lighting remained constant throughout all OCT imaging procedures at low photopic light levels (10 lux).

### **Imaging procedures**

Choroidal thickness was measured using the Spectralis OCT with EDI (Heidelberg Engineering Co, Heidelberg, Germany). This OCT device captures cross sectional images of the choroid with digital axial and transverse resolutions of  $3.9$  and  $5 \mu\text{m}$  respectively at a speed of 40,000 A-scans per second using a super luminescent diode with a central wavelength of  $870$  nm. The Automatic Real Time technology of the instrument allows for real-time compensation of eye movements and averaging of an adjustable number of B-scans ranging from 1 to 100 images. The Spectralis instrument also provides a “follow-up” function

which uses retinal landmarks as a reference for automatic registration of subsequent scans to the same location.

In this study, three sets of conventional 30° high resolution (1536 × 496 pixels per B-scan) trans-foveal EDI-OCT line scans were captured from the right eye at central, 15° nasal, and 15° temporal gaze directions in a random order (that together encompassed a region of approximately 60°) while different numbers of frames were acquired for image averaging. Gaze direction was controlled during OCT imaging by altering the position of the internal fixation targets.

To examine intrasession variations in choroidal thickness, the above scans were repeated (within 5 minutes) using the same internal fixation targets in a randomised order (Figure 1). Each scanning set included 6 consecutive 30° horizontal foveal line scans of 10, 20, 30, 40, 50 and 100 frame averaged B-scans. The first line scan of the first set for each gaze direction was always an average of 100 B-scans which was used as the reference for all subsequent scans with the follow-up imaging mode activated. With the exception of the first reference scan (which was an average of 100 B-scans), the order of the scans was randomised.

### **Regional measurements of choroidal thickness**

To obtain regional estimates of choroidal thickness, the transverse scale of the B-scans was calibrated to account for ocular magnification effects, using a previously described method<sup>20</sup> based on ocular biometry obtained using the Lenstar LS 900 optical biometer (Haag-Streit AG, Koeniz, Switzerland) and objective refraction using the Shin-Nippon NVision-K5001 open-field autorefractometer (Shin Nippon, Tokyo, Japan). The actual length of each OCT scan varied between 8.0 and 10.1 mm across all subjects, equivalent to a total combined line scan between 16 to 20 mm. These adjusted scan lengths (corrected to account for the effect of ocular magnification) were then used for regional measurements of choroidal thickness.

A custom written algorithm<sup>21</sup> was then used to automatically segment the anterior and posterior boundaries of the choroid, defined as the outer border of the hyper-reflective line corresponding to the RPE/Bruch's membrane complex and the inner border of the hyper-reflective line corresponding to the chorioscleral junction, respectively. The segmented images were visually inspected and manually corrected by a single experienced observer who was masked to the frame averaging condition to ensure that the automated segmentation accurately represented the contour of the anterior and posterior boundaries of the choroid.<sup>22</sup>

Image contrast enhancement was used to improve the visualisation of the choriocleral junction if the posterior choroidal boundary was difficult to delineate.<sup>23</sup>

The location of the fovea was manually marked in each line scan at the deepest point in the foveal pit. Given the absence of choroidal tissue within the optic nerve head, the nasal and temporal margins of the optic nerve head where Bruch's membrane terminates were marked on the B-scans intersecting the optic nerve head, and thickness data within this area were excluded. The choroidal thickness data were then extracted and averaged across the macular and extra-macular regions centred on the fovea. The macular region consisted of the foveal zone with a 1 mm diameter surrounded by the parafoveal and perifoveal eccentricities each with a 1 mm width. The extra-macular region comprised the near-peripheral and peripheral eccentricities with 1.5 mm and 3 mm widths respectively. The central B-scan was used to measure the thickness of the foveal, parafoveal, and perifoveal choroid, with average estimates of the near-peripheral and peripheral choroidal thickness calculated from the nasal and temporal B-scan data.

Choroidal thickness was calculated using the Laplace mathematical method,<sup>24</sup> to obtain more accurate thickness estimates in peripheral regions. The Laplace method also provides more precise measurement of choroidal thickness in areas where the contour of the choroidal boundary changes rapidly exhibiting an irregular non-uniform border (such as the insertion points of the ciliary arteries into the choroid and the peripapillary region).<sup>25</sup>

### **Statistical analysis**

To examine the impact of B-scan averaging upon regional measures of choroidal thickness, a repeated measures analysis of variance was carried out with three within-subject factors including the number of averaged frames (6 levels), choroidal eccentricity (5 levels), and scan order (2 levels). Significant main effects were explored with pairwise comparisons using a Bonferroni correction for multiple comparisons.

The regional choroidal thickness across the entire macular and extra-macular eccentricities was then averaged for each scanning session to obtain a single averaged wide-field choroidal thickness value across a 14 mm region centred on the fovea. To assess the intra-session variability in choroidal thickness, the Bland-Altman plot of the difference in repeated measures of wide-field choroidal thickness against the respective mean values was generated for each image averaging condition. The exact 95% confidence intervals (CI) for the upper

and lower limits of agreement (LOAs) considered as a pair were calculated.<sup>26</sup> Comparisons between the different image averaging conditions were carried out using the F-test to compare variances of the different image averaging conditions. Bland-Altman plots were also generated for repeated measures of choroidal thickness at each eccentricity to examine the impact of B-scan averaging on intrasession variations in regional measures of choroidal thickness. An F-test was then used to compare the intrasession LOAs across different image averaging conditions. This was performed separately for each choroidal eccentricity with Bonferroni correction for multiple comparisons. Further, the association between regional measures of wide-field choroidal thickness (that is the average of intrasession repeated measurements pooled across different eccentricities) and the respective intrasession repeatability was investigated using Spearman correlation for each image averaging condition. The agreement between wide-field choroidal thickness measurements obtained with each image averaging condition and the wide-field choroidal thickness with averaging 100 B-scans were also examined using Bland-Altman plots and were compared using the F-test. Additionally, the intrasession coefficient of repeatability (CR) and the 95% CI for the estimated CR<sup>27</sup> of the wide-field choroidal thickness were calculated for each image averaging condition.

## RESULTS

Repeated measures analysis of variance revealed no statistically significant differences between the mean regional choroidal thickness values obtained with the different image averaging conditions or scan order ( $p > 0.05$ ). No significant interactions were observed between the image averaging condition, the choroidal eccentricity and the order of scans for determination of the regional wide-field choroidal thickness (all  $p > 0.05$ ), suggesting that the number of frames used for B-scan averaging did not influence the mean regional estimates of wide-field choroidal thickness.

The intrasession CR and the respective 95% CI for the average wide-field choroidal thickness (i.e. the average choroidal thickness across a 14 mm region centred on the fovea) obtained with different frame averaging conditions are presented in Table 1. The Bland-Altman analyses for the intrasession repeatability of the average wide-field choroidal thickness for different image averaging conditions were compiled in Figure 2. The intrasession repeatability of the average wide-field choroidal thickness did not vary significantly across

different image averaging conditions following Bonferroni correction for multiple comparisons (all  $p > 0.01$ ).

To further explore the interaction between the B-scan averaging condition, intrasession repeatability of choroidal thickness, and choroidal eccentricity, the Bland-Altman graphs for intrasession repeated measures of choroidal thickness at each eccentricity using the different image averaging conditions were plotted in Figure 3. The intrasession variability in measures of choroidal thickness at the fovea reduced as the number of frames used for B-scan averaging increased from 10 to 100 frames, with the improvement in intrasession repeatability value approaching statistical significance when 40 (mean difference  $-3 \pm 8 \mu\text{m}$ ) or 100 (mean difference  $-5 \pm 7 \mu\text{m}$ ) B-scans were averaged compared to averaging 10 B-scans (mean difference  $-1 \pm 13 \mu\text{m}$ ) ( $p=0.03$  for both comparisons). The variability in repeated measures of choroidal thickness in other eccentricities beyond the fovea did not vary significantly between the B-scan averaging conditions. The association between the regional measures of wide-field choroidal thickness and the intrasession repeatability was only significant when 10 B-scans were averaged ( $r = 0.63$ ,  $p < 0.001$ ;  $p > 0.05$  for all other higher B-scan averaging conditions  $> 10$  B-scans), with increased choroidal thickness associated with a greater intrasession variability.

A comparison of the Bland-Altman analyses for the agreement of the average wide-field choroidal thickness using different image averaging conditions and that obtained using 100 averaged B-scans (assuming that 100 averaged B-scans provided the most reliable estimate of the choroidal thickness due to improved visibility of the posterior choroidal boundary) is displayed in Figure 4. The LOAs between the mean wide-field choroidal thickness using 10 and 100 averaged B-scans (mean difference  $2 \pm 5 \mu\text{m}$ , 95% LOAs  $+13$  to  $-8 \mu\text{m}$ ) were significantly larger (i.e. lower agreement) than the LOAs of the same measurements using 50 and 100 averaged B-scans (mean difference  $1 \pm 2 \mu\text{m}$ , 95% LOAs  $+6$  to  $-3 \mu\text{m}$ ) ( $p < 0.01$  with Bonferroni correction). Further, the difference in the agreement of the average wide-field choroidal thickness using 20 versus 100 frame averaged B-scans (mean difference  $3 \pm 6 \mu\text{m}$ , 95% LOAs  $+13$  to  $-6 \mu\text{m}$ ) and 50 versus 100 frame averaged B-scans (mean difference  $1 \pm 2 \mu\text{m}$ , 95% LOAs  $+6$  to  $-3 \mu\text{m}$ ) approached statistical significance ( $p=0.02$ ). No statistically significant difference was found between the agreement of the average wide-field choroidal thickness measurement using 30 versus 100 (mean difference  $2 \pm 4 \mu\text{m}$ , 95% LOAs  $+10$  to  $-7 \mu\text{m}$ ) and the agreement results using either conditions of 40 (mean difference,  $0 \pm 4 \mu\text{m}$ , 95%

LOAs +7 to -7  $\mu\text{m}$ ) and 50 (mean difference  $1 \pm 2 \mu\text{m}$ , 95% LOAs +6 to -3  $\mu\text{m}$ ) versus 100 averaged B-scans ( $p > 0.01$  for all comparisons).

## DISCUSSION

This study provides the first evidence demonstrating the optimal number of B-scans required for frame averaging to acquire repeatable and accurate measures of wide-field choroidal thickness using EDI-OCT imaging in young subjects with healthy eyes. While the short-term variability in measures of foveal choroidal thickness appeared to be influenced by the number of B-scans averaged, with a minimum of 20 frames required for B-scan averaging to obtain intrasession repeatability values comparable to that of 100 averaged B-scans, the intrasession repeatability of choroidal thickness beyond the fovea did not vary significantly across the B-scan averaging conditions. Using 30, 40, or 50 B-scans for frame averaging to estimate the average wide-field choroidal thickness improved the agreement with measurements obtained using 100 averaged B-scans (compared to using 10 or 20 averaged B-scans), suggesting that frame-averaged images comprising a minimum of 30 B-scans are required in order to achieve accurate measures of wide-field choroidal thickness.

Given the lack of consensus regarding the optimum number of frames for B-scan averaging, previous studies of choroidal thickness have employed a wide range of B-scan frames for averaging. While the majority of variations in thickness of the choroid observed across studies can be explained by differences between samples in terms of age, gender, refractive error, axial length, and measurement region,<sup>1</sup> the implementation of various OCT imaging protocols may also influence the between-study variations in choroidal thickness.<sup>28</sup> Estimates of choroidal thickness may be affected by the number of frames used for B-scan averaging due to the smoothing effect and improved visibility of the posterior border of the choroid associated with image averaging.<sup>29</sup> In the healthy young adults participating in this study, however, no evidence of significant change in regional estimates of wide-field choroidal thickness was found across a 60° area associated with the number of frames used for B-scan averaging, suggesting that using a different number of frames for B-scan averaging during EDI-OCT imaging does not introduce a significant bias in measurements of choroidal thickness. Previous studies examining the effect of B-scan averaging on retinal thickness also support this finding, with the average retinal thickness values unaffected by the number of B-scans averaged.<sup>30</sup>

The intrasession repeatability did not vary significantly across the B-scan averaging conditions, with intrasession CR of the average wide-field choroidal thickness ranging from 5 to 9  $\mu\text{m}$  (95% CI 3 to 14  $\mu\text{m}$ ). Similarly, beyond the foveal region, intrasession repeatability did not vary significantly across the different image averaging conditions. However, the repeatability of foveal choroidal thickness progressively improved with increasing numbers of B-scans, with short-term variability reducing by approximately half when 40 (CR 13, 95% CI 7 to 20  $\mu\text{m}$ ) or 100 B-scans (CR 13, 95% CI 6 to 19  $\mu\text{m}$ ) were averaged compared to 10 B-scans (CR: 25, 95% CI: 13 to 37  $\mu\text{m}$ ). The reduced visibility of the chorioscleral junction due to the typically greater thickness of the sub-foveal choroid<sup>31</sup> may contribute to the increased variability of the sub-foveal choroidal thickness when measures are obtained from an average of only 10 B-scans. This is further supported by the significant association found between the choroidal thickness and the intrasession variability when 10 B-scans were used for frame averaging, whereas the regional variations in choroidal thickness were not correlated with intrasession repeatability in the other higher frame averaging conditions (that is 20 to 100 B-scans). Therefore, a minimum of 20 B-scans may be required for frame averaging during EDI-OCT choroidal imaging, particularly for the foveal region, with intrasession reliability expected to compare favourably with that of 100 averaged B scans.

Short-term variations in the thickness of choroid between repeated scans within 3 hours have been investigated previously using 1 to 100 frames to derive an averaged B-scan image of the choroid, with intrasession repeatability of choroidal thickness varying from 4 to 45  $\mu\text{m}$ .<sup>32-37</sup> The magnitude of intrasession repeatability of average wide-field choroidal thickness found in this study (intrasession CR 5 to 9, 95% CI 3 to 14  $\mu\text{m}$ ) using different B-scan averaging conditions is consistent with Read et al.<sup>35</sup> and Twa et al.<sup>36</sup> who reported that macular choroidal thickness varied by approximately 4 to 15  $\mu\text{m}$  within an hour, using the Spectralis instrument and averaging of 30 to 35 B-scans. Mansouri et al.,<sup>34</sup> however, demonstrated that consecutive measures of choroidal thickness averaged across a 12-mm foveal line scan vary by approximately 45  $\mu\text{m}$  using a prototype swept-source OCT instrument capable of averaging up to 96 frames. Similarly, Rahman et al.<sup>37</sup> reported the intrasession repeatability of foveal choroidal thickness to be approximately 37  $\mu\text{m}$ . Given the lack of real-time retinal tracking technology in these studies,<sup>34, 37</sup> the greater intrasession variability reported may partly be explained by variations in scan positioning across the measurement sessions.

The change in the accuracy of choroidal thickness measurements was also examined by comparing the agreement between the mean wide-field choroidal thickness using an average

of 100 B-scans and each of the 10, 20, 30, 40, or 50 frame-averaged images, assuming that the best estimate of the actual choroidal thickness would be obtained using the average of 100 B-scans with maximum enhancement of the visibility of the anterior and posterior boundaries of the choroid. Furthermore, the thickness of the choroid varies periodically with ocular pulsation occurring every 0.8 to 1.3 seconds,<sup>38,39</sup> thus the longer scan acquisition associated with averaging 100 B-scans would provide sufficient time to obtain the average choroidal thickness across a minimum of an entire ocular pulse cycle. The accuracy of choroidal thickness measures improved progressively as the number of B-scans used for frame averaging increased, with the estimate of choroidal thickness using 10 B-scans for frame averaging (95% LOAs +13 to -8  $\mu\text{m}$ ) exhibiting a significantly lower accuracy (i.e. greater variability with wider LOAs) compared to that of 50 averaged B-scans (95% LOAs +6 to -3  $\mu\text{m}$ ) ( $p < 0.01$ ), and also a marginally significant lower accuracy was found in measures of choroidal thickness with averaging of 20 B-scans (95% LOAs +13 to -6  $\mu\text{m}$ ) compared to that of 50 averaged B-scans ( $p < 0.02$ ). However, the choroidal thickness measurements using an average of 30 (95% LOAs +10 to -7  $\mu\text{m}$ ), 40 (95% LOAs +7 to -7  $\mu\text{m}$ ), or 50 B-scans (95% LOAs +6 to -3  $\mu\text{m}$ ) exhibited similar agreement to the choroidal thickness estimate from 100 averaged B-scans. These results suggest that a minimum of 30 B-scans are required for frame averaging to accurately estimate the thickness of the choroid.

The results from this study may not be generalisable to older subjects with media opacity, reduced vision, or unstable fixation, particularly given the recent report suggesting the need for averaging a greater number of B-scans in the presence of media opacity to improve image quality of retinal OCT images.<sup>10</sup> Further, the optimum number of B-scans required for averaging may vary for determination of the thickness of different vascular layers of the choroid, given the potential confounding effect of background noise on the threshold levels for binarization techniques that are often used in these measurements.<sup>40</sup> Our study was also limited by the small number of subjects examined which may have reduced the power to detect statistically significant differences in choroidal thickness across different image averaging conditions. However, the variation in regional measures of choroidal thickness across the examined B-scan averaging conditions was less than 6  $\mu\text{m}$ , which is close to the axial resolution of the majority of commercially available OCT instruments and has minimal clinical significance.

## CONCLUSION

In this study, altering the number of averaged B-scans did not introduce a systematic bias for regional measures of wide-field choroidal thickness, and averaging more than 10 B-scans did not significantly enhance the clinical identification of the choroid using EDI-OCT imaging in this sample of healthy young adults. However, the repeatability and accuracy of choroidal thickness measurements were influenced by B-scan averaging. A minimum of 30 B-scans in each individual line scan was required for accurate measures of regional choroidal thickness across a 60° area, with the magnitude of improvement in accuracy of the choroidal thickness estimates using greater than 30 B-scans being negligible in this population.

## REFERENCES

1. Regatieri CV, Branchini L, Fujimoto JG, et al. Choroidal imaging using spectral-domain optical coherence tomography. *Retina* 2012;32:865-876.
2. Park JY, Kim BG, Hwang JH, et al. Choroidal thickness in and outside of vascular arcade in healthy eyes using spectral-domain optical coherence tomography. *Invest Ophthalmol Vis Sci.* 2017;58:5827-5837.
3. Mohler KJ, Draxinger W, Klein T, et al. Combined 60° wide-field choroidal thickness maps and high-definition en face vasculature visualization using swept-source megahertz OCT at 1050 nm. *Invest Ophthalmol Vis Sci.* 2015;56:6284-6293.
4. Hoseini-Yazdi H, Vincent S, Collins MJ, et al. Wide-field choroidal thickness in myopes and emmetropes. *Invest Ophthalmol Vis Sci.* 2017;58:1108.
5. Pang CE, Shah VP, Sarraf D, et al. Ultra-widefield imaging with autofluorescence and indocyanine green angiography in central serous chorioretinopathy. *Am J Ophthalmol.* 2014;158:362-371.
6. Zhang C, Tatham AJ, Medeiros FA, et al. Assessment of choroidal thickness in healthy and glaucomatous eyes using swept source optical coherence tomography. *PLoS One.* 2014;9:e109683.
7. Alonso-Caneiro D, Read SA, Collins MJ. Speckle reduction in optical coherence tomography imaging by affine-motion image registration. *J Biomed Opt.* 2011;16:116027-1160275.
8. Shirasawa M, Sakamoto T, Terasaki H, et al. Objective determination of optimal number of spectral-domain optical coherence tomographic images of retina to average. *PLoS One.* 2014;9:e110550.

9. Wu W, Tan O, Pappuru RR, et al. Assessment of frame-averaging algorithms in OCT image analysis. *Ophthalmic Surg Lasers Imaging Retina*. 2013;44:168-175.
10. Podkowinski D, Sharian Varnousfaderani E, Simader C, et al. Impact of B-Scan averaging on Spectralis optical coherence tomography image quality before and after cataract surgery. *J Ophthalmol*. 2017;2017: 8148047.
11. Sakamoto A, Hangai M, Yoshimura N. Spectral-domain optical coherence tomography with multiple B-scan averaging for enhanced imaging of retinal diseases. *Ophthalmology*. 2008;115:1071-1078.
12. El-Shazly A, Farweez Y, Elzankalony YA, et al. Effect of smoking on macular function and structure in active smokers versus passive smokers. *Retina* 2017;doi: 10.1097/IAE.0000000000001632.
13. Vural AD, Kara N, Sayin N, et al. Choroidal thickness changes after a single administration of coffee in healthy subjects. *Retina*. 2014;34:1223-1228.
14. Kang HM, Woo YJ, Koh HJ, et al. The effect of consumption of ethanol on subfoveal choroidal thickness in acute phase. *Br J Ophthalmol*. 2016;100:383-388.
15. Chen Z, Xue F, Zhou J, et al. Effects of orthokeratology on choroidal thickness and axial length. *Optom Vis Sci*. 2016;93:1064-1071.
16. Zhang Z, Zhou Y, Xie Z, et al. The effect of topical atropine on the choroidal thickness of healthy children. *Sci Rep*. 2016;6:34936.
17. Woodman-Pieterse EC, Read SA, Collins MJ, et al. Regional changes in choroidal thickness associated with accommodation. *Invest Ophthalmol Vis Sci*. 2015;56:6414-6422.
18. Read SA, Collins MJ. The short-term influence of exercise on axial length and intraocular pressure. *Eye*. 2011;25:767-774.
19. Read SA. Ocular and environmental factors associated with eye growth in childhood. *Optom Vis Sci*. 2016;93:1031-1041.
20. Read SA, Collins MJ, Vincent SJ, et al. Choroidal thickness in myopic and nonmyopic children assessed with enhanced depth imaging optical coherence tomography. *Invest Ophthalmol Vis Sci*. 2013;54:7578-7586.
21. Alonso-Caneiro D, Read SA, Collins MJ. Automatic segmentation of choroidal thickness in optical coherence tomography. *Biomed Opt Express*. 2013;4:2795-2812.
22. Read SA, Collins MJ, Vincent SJ, et al. Choroidal thickness in childhood. *Invest Ophthalmol Vis Sci*. 2013;54:3586-3593.

23. Girard MJ, Strouthidis NG, Ethier CR, et al. Shadow removal and contrast enhancement in optical coherence tomography images of the human optic nerve head. *Invest Ophthalmol Vis Sci.* 2011;52:7738-7748.
24. Jones SE, Buchbinder BR, Aharon I. Three-dimensional mapping of cortical thickness using Laplace's Equation. *Hum Brain Mapp.* 2000;11:12-32.
25. Alonso-Caneiro D, Read SA, Vincent SJ, et al. Tissue thickness calculation in ocular optical coherence tomography. *Biomed Opt Express.* 2016;7:629-645.
26. Carkeet A. Exact parametric confidence intervals for Bland-Altman limits of agreement. *Optom Vis Sci.* 2015;92:e71-e80.
27. Bland JM. What is the standard error of the within-subject standard deviation, sw? 2011. Available from: <https://www-users.york.ac.uk/~mb55/meas/seofsw.htm>.
28. Chhablani J, Barteselli G, Bartsch D-U, et al. Influence of scanning density on macular choroidal volume measurement using spectral-domain optical coherence tomography. *Graefes Arch Clin Exp Ophthalmol.* 2013;251:1303-1309.
29. Philip A-M, Gerendas BS, Zhang L, et al. Choroidal thickness maps from spectral domain and swept source optical coherence tomography: algorithmic versus ground truth annotation. *Br J Ophthalmol.* 2016;100:1372-1376.
30. Giani A, Deiro AP, Staurenghi G. Repeatability and reproducibility of retinal thickness measurements with spectral-domain optical coherence tomography using different scan parameters. *Retina.* 2012;32:1007-1012.
31. Cho A, Choi Y, Kim Y. Influence of choroidal thickness on subfoveal choroidal thickness measurement repeatability using enhanced depth imaging optical coherence tomography. *Eye.* 2014;28:1151-1160.
32. Yamashita T, Yamashita T, Shirasawa M, et al. Repeatability and reproducibility of subfoveal choroidal thickness in normal eyes of Japanese using different SD-OCT devices. *Invest Ophthalmol Vis Sci.* 2012;53:1102-1107.
33. Gupta P, Jing T, Marziliano P, et al. Distribution and determinants of choroidal thickness and volume using automated segmentation software in a population-based study. *Am J Ophthalmol.* 2015;159:293-301.
34. Mansouri K, Medeiros FA, Tatham AJ, et al. Evaluation of retinal and choroidal thickness by swept-source optical coherence tomography: repeatability and assessment of artifacts. *Am J Ophthalmol.* 2014;157:1022-1032.
35. Read SA, Alonso-Caneiro D, Vincent SJ, et al. Longitudinal changes in choroidal thickness and eye growth in childhood. *Invest Ophthalmol Vis Sci.* 2015;56:3103-3112.

36. Twa MD, Schulle KL, Chiu SJ, et al. Validation of macular choroidal thickness measurements from automated SD-OCT image segmentation. *Optom Vis Sci.* 2016;93:1387-1398.
37. Rahman W, Chen FK, Yeoh J, et al. Repeatability of manual subfoveal choroidal thickness measurements in healthy subjects using the technique of enhanced depth imaging optical coherence tomography. *Invest Ophthalmol Vis Sci.* 2011;52:2267-2271.
38. Kaufmann C, Bachmann LM, Robert YC, et al. Ocular pulse amplitude in healthy subjects as measured by dynamic contour tonometry. *Arch Ophthalmol.* 2006;124:1104-1108.
39. Butt Z, O'Brien C. Reproducibility of pulsatile ocular blood flow measurements. *J Glaucoma.* 1995;4:214-218.
40. Uji A, Balasubramanian S, Lei J, et al. Impact of multiple En face image averaging on quantitative assessment from optical coherence tomography angiography images. *Ophthalmology.* 2017;124:944-952.

Corresponding author name and e-mail address: Hosein Hoseini-Yazdi, Contact Lens and Visual Optics Laboratory, School of Optometry and Vision Science, Queensland University of Technology, Room B561, O Block, Victoria Park Road, Kelvin Grove 4059, Brisbane, Queensland, Australia. Email: s.hoseiniyazdi@qut.edu.au

**Table 1:** Intrasection repeatability of averaged wide-field choroidal thickness measurements using different numbers of frames for B-scan averaging

| <b>Number of Averaged B-scans</b> | <b>Mean (SD) Relative Difference Between Repeated Measures (<math>\mu\text{m}</math>)</b> | <b>Mean (SD) Absolute Difference Between Repeated Measures (<math>\mu\text{m}</math>)</b> | <b>Intrasection CR (<math>\mu\text{m}</math>)</b> | <b>95% CI for Intrasection CR (<math>\mu\text{m}</math>)</b> |
|-----------------------------------|---|---|---|--|
| <b>10</b>                         | -1 (4)  | 3 (2)   | 8   | 4 – 11   |
| <b>20</b>                         | -2 (5)  | 4 (3)   | 9   | 5 – 14   |
| <b>30</b>                         | -1 (4)  | 3 (1)   | 7   | 3 – 10   |
| <b>40</b>                         | -1 (4)  | 3 (2)   | 7   | 4 – 11   |
| <b>50</b>                         | -3 (4)  | 4 (3)   | 9   | 4 – 13   |
| <b>100</b>                        | -2 (3)  | 2 (2)   | 5   | 3 – 8  |

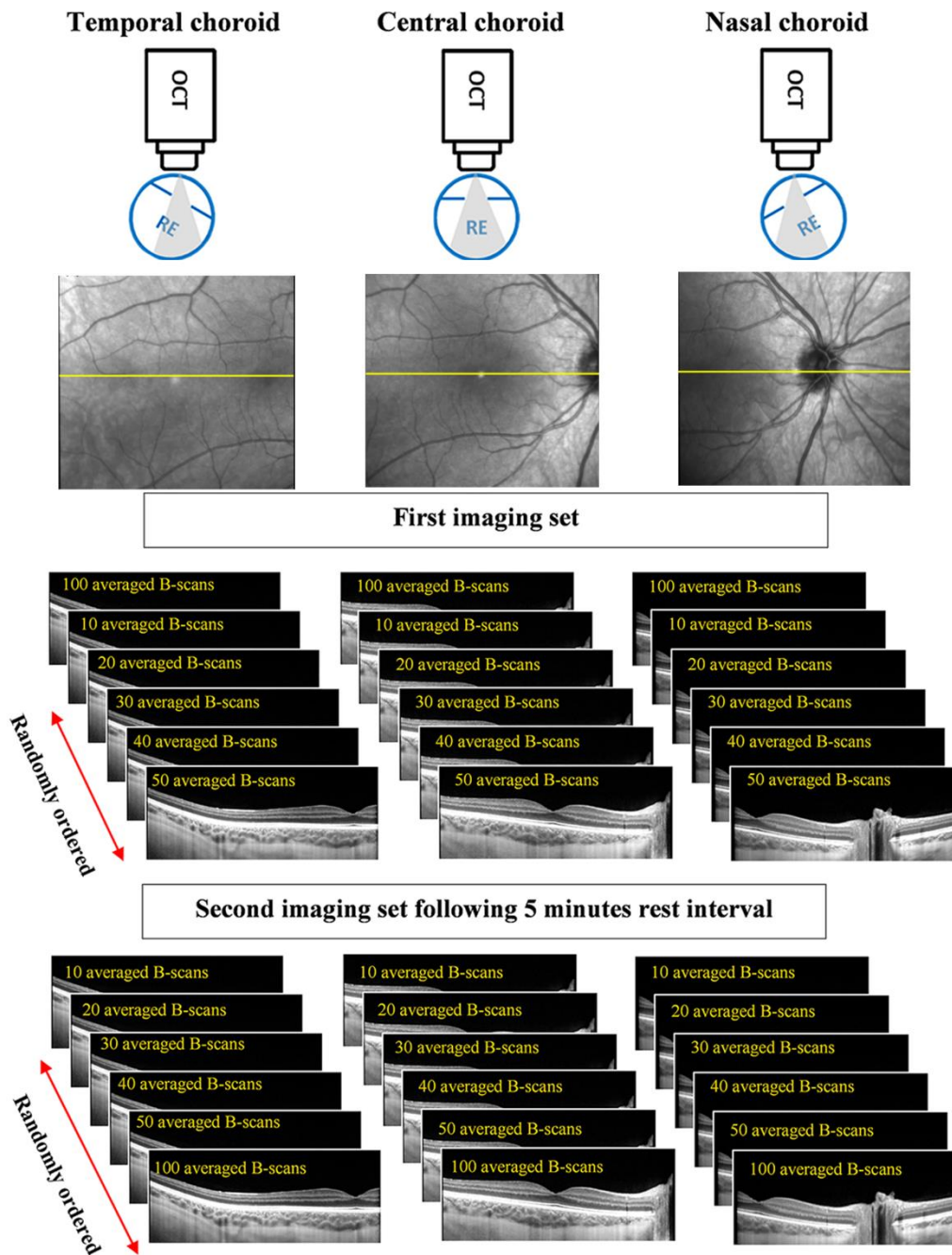


**Figure 1:** Diagram of the scanning protocol employed in this study. Two sets of horizontal trans-foveal EDI-OCT line scans encompassing a  $30^\circ$  area of the temporal, central, and nasal choroid (through  $15^\circ$  changes in gaze direction) of the right eye were acquired, which were separated by a 5-minute rest interval while the left eye was occluded. For each OCT imaging set and gaze direction, different numbers of B-scans were averaged including 10, 20, 30, 40, 50, and 100 B-scans. While the first B-scan acquired at each gaze direction during the first OCT imaging set was an average of 100 B-scans, the order of the remaining B-scans was randomised. RE, right eye

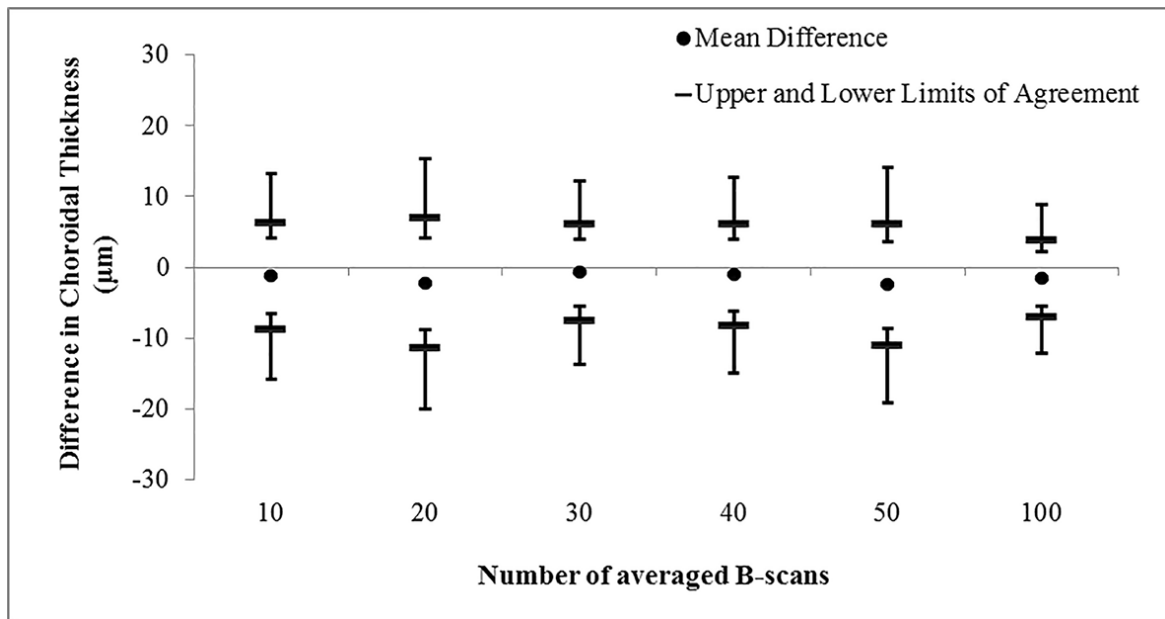


**Figure 2:** Intrasession repeatability of the average wide-field choroidal thickness (averaged across all eccentricities) with different numbers of averaged B-scans. The error bars represent the exact 95% confidence intervals for the upper and lower limits of agreement between repeated measures.

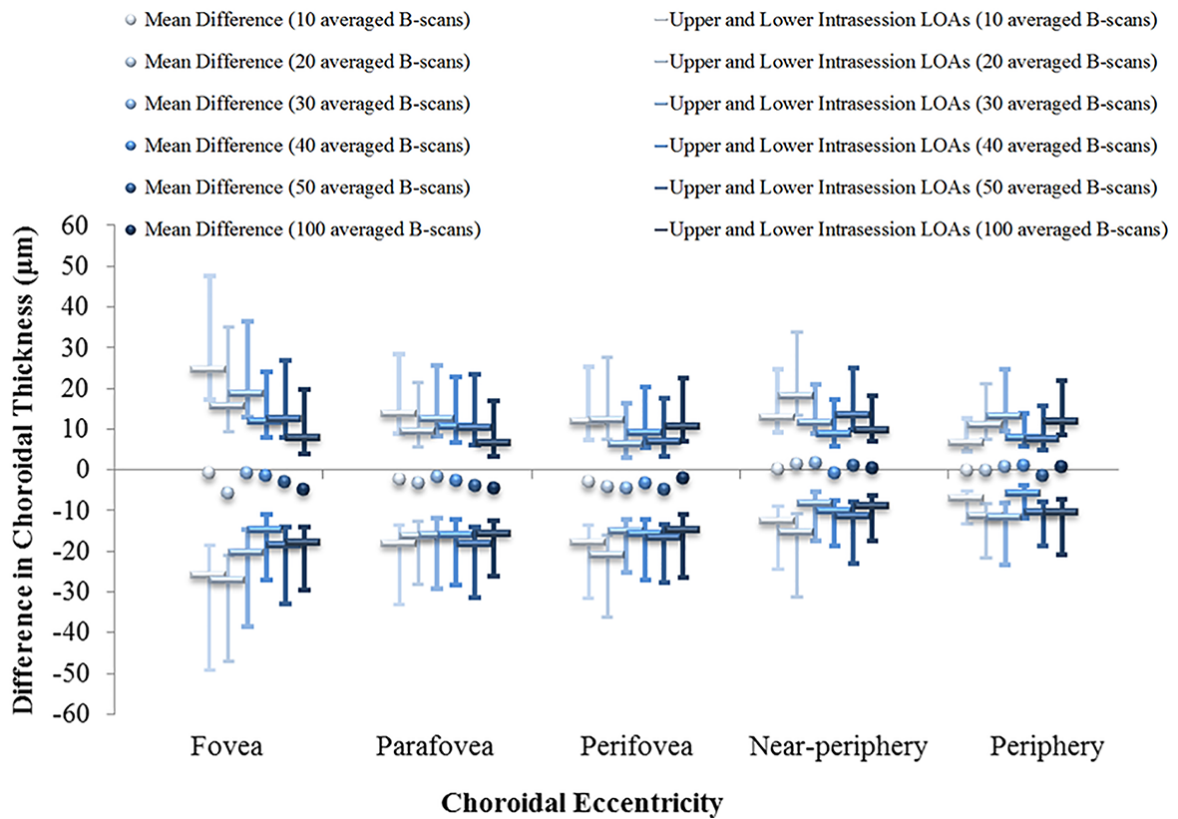


**Figure 3:** Intrasession repeatability of the choroidal thickness with different numbers of averaged B-scans at various eccentricities within the central 60° area of the fundus. The error bars represent the exact 95% confidence intervals for the upper and lower limits of agreement.

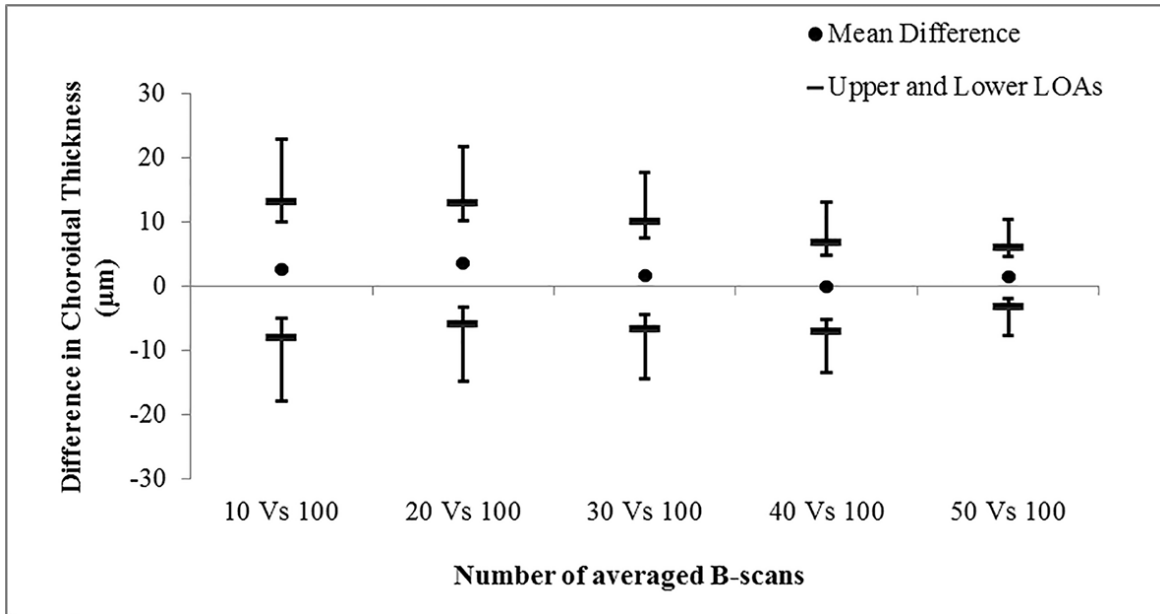


**Figure 4:** Comparison of the Bland-Altman analyses for the agreement of the average wide-field choroidal thickness measurement using different numbers of averaged B-scans versus 100 averaged B-scans. Error bars represent the exact 95% confidence intervals for the upper and lower limits of agreement.